Monte Carlo simulations and self-consistent field theory applied to calculations of density profiles in A1BA2 triblock copolymer melts*)

Michał Dzięcielski[1)], Sebastian Wołoszczuk[1)], Michał Banaszak[1),)]**

DOI: dx.doi.org/10.14314/polimery.2014.580

Abstract: Using two complementary numerical methods, the lattice Monte Carlo simulations with parallel tempering and self-consistent field theory, we investigate the distribution of A1, B, and A2 segments in the lamellar nanostructure of A1BA2 triblock copolymer melts. While the lattice Monte Carlo method is in principle exact, it is limited by a variety of factors, such as finite size effects, long relaxation times required to reach the thermal equilibrium and geometry of the underlying lattice. It is also limited to chains consisting of relatively few segments. The self-consistent field theory, on the other hand, is free of the above limitations, but it is a mean-field approach which does not take into account the thermal fluctuations. Therefore we confront the results obtained from the two above methods and draw conclusions concerning both the comparison of the two methods and the localization of the A1 segments in the B domain with increasing length of the A1 block. For Monte Carlo simulations we employ two types of chains, 2-32-30 and 1-16-15, and for the self-consistent field theory we use the corresponding values of the thermodynamic incompatibility parameter, χN.

Keywords: diblock copolymers, density profiles, self-consistent field theory, molecular modeling, Monte Carlo simulation.

Symulacje Monte Carlo i teoria pola samozgodnego stosowane do obliczeń profilów gęstości w stopach trójblokowych kopolimerów A1BA2

Streszczenie: Teorię samozgodnego pola średniego i symulacje Monte Carlo wykorzystano do oceny dystrybucji segmentów A1, B i A2 w strukturach warstwowych. Porównano wyniki uzyskane za pomocą tych dwóch metod i przedstawiono wnioski dotyczące zmian lokalizacji segmentów A1 w domenie B wraz ze zwiększaniem długości bloków A1.

Słowa kluczowe: kopolimery dwublokowe, profile gęstości, teoria pola samozgodnego, modelowanie molekularne, symulacje Monte Carlo.

Separations in block copolymer melts lead to self-assemblies into a variety of nanostructures [1]. A linear triblock ABC copolymer chain consists, in general, of three distinct blocks, A, B, and C, connected sequentially. Terminal blocks A and C are often built from the same type of segment, resulting in a triblock copolymer A1BA2 which has only 2 types of segments, A and B, as the diblock. In this paper we focus on such A1BA2 triblocks. While AB diblock copolymer melts are known to form only a few stable nanophases {such as layers (L), hexagonally packed cylinders (C), gyroid nanostructures (G), with the Ia3d symmetry, cubically packed spherical cells (S), and a recently reported O^{70}-phase [2, 3]}, the triblock melts form tens of different phases [1]. In case of a diblock AB copolymer melt, the phase behavior is controlled by the chain composition, volume fraction of segments of type A — f, degree of polymerization (total number of segments — N) and the temperature-related parameter — χ [4, 5]. The ordered nanophase can be dissolved into a disordered phase, for example, upon heating. Phase diagrams of such melts exhibiting order-disorder transition (ODT) lines and order-order transition (OOT) lines are known from experiments [6] and are successfully predicted by mean-field (MF) theories [7, 8], such as self-consistent field theory (SCFT) which is based on the standard Gaussian chain model [9], or theories including fluctuations [10, 11]. The MF phase behavior of the A1BA2 triblock melt is governed by χN [1] and the triblock composition, f_{A1}, $f_{B,}$ and $f_{A2,}$ where $f_B = 1/2$, $f_{A1} + f_B + f_{A2} = 1$. Since the amount of B segments is equal to that of A segments,

[1)] A. Mickiewicz University, Faculty of Physics, ul. Umultowska 85, 61-614 Poznan, Poland.

*) Material contained in this article was presented at the IX International Conference "X-Ray investigations of polymer structure", Zakopane, Poland, 3—6 December 2013.

**) Author for correspondence; e-mail: michal.banaszak@amu.edu.pl

a lamellar phase is expected. But the arrangement of the copolymer chain is not obvious. The interesting effect is localization of the short A1 blocks. This localization is a result of competition of enthalpic and entropic effects. Enthalpy would favor demixing of A and B segments, and since the short A1 block is always close to the B segments, the A1 blocks would go to the A-B interface (between A domain and B domain). Anchoring the A1 block to the interface reduces the entropy of the copolymer chain, therefore from the entropic point of view, it may be more favorable to place the A1 block within the B domain. Which effect is more significant depends both on f_{A1} and χN (Matsen's theory). For small f_{A1} the entropic effects should dominate, and therefore the A1 blocks are localized in the B domain. This is supported by both Monte Carlo (MC) and SCFT. The purpose of this paper is to confront the MC and SCFT data concerning the density profiles in the lamellar phase. In previous studies [12, 13] we established a relation between the MC and SCFT data concerning the phase behavior. In this paper we intend to investigate the relation between the MC and SCFT density profiles.

METHODOLOGY

Self-consistent field theory

Self-consistent field theory was successfully applied to the block copolymer melts [8, 14, 15]. It enables a relatively fast and accurate calculation of phase diagrams corresponding to diagrams obtained experimentally. The SCFT approach is based on the assumption that coarse-grained polymer chains in dense melts are Gaussian (Flory's theorem), and on the mean-field approximation which selects the dominant contribution in the appropriate partition function, thus neglecting fluctuations. In this method we go from particles to fields using modified diffusion equations. It exists in many variations, both in real space (*r*-space) [16] and Fourier space (*k*-space) [17]. While *k*-versions of the SCFT are more successful in predicting the non-classical gyroid phases, we will mostly use the *r*-version, based on the unit cell approximation (UCA) [18] method. In this approach, periodic nanophase is approximated by a *D* dimensional sphere, where $D = 1$, 2, and 3, corresponding to lamellar, cylindrical and spherical nanophases. To solve iteratively the modified diffusion equations until the self-consistency condition is met, we use the Crank-Nicholson scheme. Next we calculate the reduced free energy *F* (per chain in k_BT units). Numerically, we find *R* which minimizes *F*:

$$\frac{F(R,D)}{nk_BT} = -\ln\frac{Q}{V} + \frac{D}{R^D\int_0^R r^{D-1}}\left[N\chi\left(\varphi_{A_1}+\varphi_{A_2}\right)\varphi_B - \right.$$
$$\left. -W_A\left(\varphi_{A_1}+\varphi_{A_2}\right) - W_B\varphi_B\right] \quad (1)$$

where: Q — the partition function of a single Gaussian chain in external fields W_A and W_B acting on segments A and B, respectively; V — volume in which n diblock chains are confined and φ_{A1}, φ_B, φ_{A2} are density profiles. When the difference between F and F_{dis} (free energy of the disordered phase) is negative then the appropriate nanophase is thermodynamically stable in the point considered (χN, f). Otherwise the system comprises the disordered phase. As a result of calculations we have also density profiles of segments φ_{A1}, φ_{A2} and φ_B in the direction normal to layers. Note that we use the following normalization of the density profiles:

$$\varphi_{A_1}(x) + \varphi_{A_2}(x) + \varphi_B(x) = 1 \quad (2)$$

where x — coordinate normal to layers.

Monte Carlo

The simulations are performed using cooperative motion algorithm (CMA) [19] for a face-centered cubic (FCC) lattice with the coordination number $z = 12$ and the bond length $\sqrt{2}a$, where a is the FCC lattice constant. Chain bonds are not allowed to be broken or stretched and the usual periodic boundary conditions are applied. The lattice box size is chosen to fit the chain, and the lattice sites are completely filled with chain segments — there are no vacancies. Since all lattice sites are occupied, a chain segment can move if other segments move simultaneously. An attempt to move a single segment defines a single Monte Carlo step. The interaction energy between segments of types i and j is given by ε_{ij}, with $\varepsilon_{AA} = \varepsilon_{BB} = 0$ and $\varepsilon_{AB} = \varepsilon$. The interaction is limited to the nearest neighbors ($z = 12$), and the interaction parameter, ε, is related to the Flory parameter by the following equation:

$$\chi = \frac{(z-2)\varepsilon}{kT} \quad (3)$$

The reduced energy per lattice site and the reduced temperature are defined as follows:

$$\frac{E^\bullet}{n_\alpha} = \frac{\frac{E}{\varepsilon}}{n_\alpha} \quad (4)$$

$$T^\bullet = \frac{kT}{\varepsilon} \quad (5)$$

where n_α — the number of lattice sites.

Relation between reduced temperature and the χ parameter is

$$\chi N = \frac{N\zeta}{T^\bullet} \quad (6)$$

In this paper the value of ζ is set to 7.5, as justified in ref. [20]. We start the simulation by equilibrating the system in the athermal limit, that is, where ε/kT is zero. When the system reaches its thermal equilibrium, the polymer chains assume statistical conformations, random orientations, and become uniformly distributed within the simulation box. We record the translational diffusion of the copolymer chains in order to estimate the simulation time scale. In the athermal melt, it takes about $1.4\cdot10^4$ MC timesteps to diffuse at a distance of the order of the radius of gyration of the copolymer chain. We equi-

librate the athermal melt for 10^7 MC timesteps, and from the equilibrated melt state the system is quenched to a required temperature. We also verify the quality of thermal equilibration by heating the system up and cooling it down again. This procedure is fully described in [21]. For each temperature we perform $3 \cdot 10^6$ Monte Carlo (MC) timesteps. First $2 \cdot 10^6$ are to equilibrate the system, and latter $3 \cdot 10^6$ to sample the data. For a given T^* we repeat the simulation experiment six times starting with different initial states. For a given state point, all runs yield the same type of nanostructure, and the results are averaged over all such runs. While this method works relatively well for high temperatures, it tends to generate long relaxation times for lower temperatures. This results in unreliable estimates of the sampled properties. To solve this problem many modifications to the standard methods were proposed, such as parallel tempering (PT) method, in which by parallel simulation of many replicas in the relevant temperature range, the energy barriers of the local free energy minima can be overcome [22, 23]. In this paper we simulate systems from $T^* = 1$ to $T^* = 10$ at 36 different temperatures using the PT method.

RESULTS AND DISCUSSION

We simulate the A1BA2 triblock melt, using the PT method, with chain lengths $N = 64$ (see Fig. 1) and $N = 32$, with compositions as follows: $f_{A1} = 2/64$, $f_B = 32/64$ and $f_{A2} = 30/64$ on the 64×64×64 lattice and the 32×32×32 lattice.

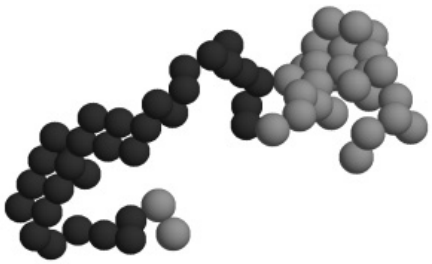

Fig. 1. Schematic picture of the 2-32-30 triblock chain; the A segments are indicated with lighter shade and the B segments are darker

While simulations for the 2-32-30 melt are performed for 36 different T^*'s from 1 to 10, we focus our attention on three representative temperatures $T^* = 3$, 4 and 7, which correspond to $\chi N = 160$, 120, and 69, respectively (with the $\chi = 7.5/T^*$ mapping) for the SCFT calculations. A typical snapshot from MC simulation is shown in Fig. 2.

As stated earlier the purpose of this paper is to demonstrate how the A1 block is distributed in the lamellar nanostructure of the A1BA2 triblock melt. This distribution clearly depends on the asymmetry, quantified by f_{A1}, thermodynamic incompatibility, quantified by χN, and (for the MC simulations) also on the chain length, N.

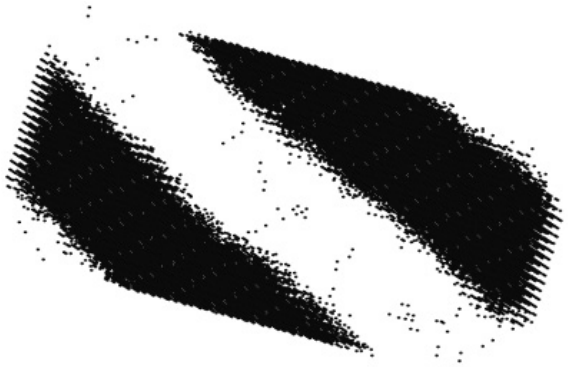

Fig. 2. Snapshot of the lamellar structure of the 2-32-30 triblock melt at $T^* = 3$; for clarity only the A segments are shown and the B segments are not shown; note the A1 segments that are localized in the B domain

From diblock studies it is known that below the order-disorder transition temperature the A domain and the B domain are separated by an interface which contains the junctions between A block and B block.

Similarly, for the triblock the A1B and A2B junctions are expected to be localized in vicinity of the interface. However, as demonstrated previous studies [11, 12], that is not always the case because for a short A1 block can be localized within the B domain due to an entropic advantage. From concentration profiles of A1, A2, and B, as shown in Figs 3, 4, and 5 for representative cases, we estimate the fraction of the A1 blocks both in the interface and in the domain.

For example, in Fig. 5 we show the concentration profiles from the MC for $N = 64$, $T^* = 7$, and at $f_{A1} = 2/64$ and from the SCFT for corresponding $\chi N = 69$. In this case we can clearly see that the number of segments in the interface is similar to that in the B domain. It is evident that as we increase χN, more A1 segments are localized at the interface, and less in the B domain, as expected from previous studies. It is also quite interesting that the density

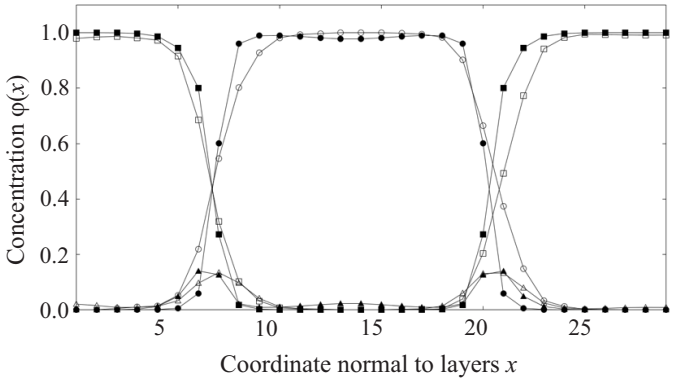

Fig. 3. Density profiles from MC simulations for the 2-32-30 melt: A1 blocks — (Δ), B blocks — (○), A2 blocks — (□) and SCFT calculations: A1 blocks — (▲), B blocks — (●), A2 blocks — (■); $T^* = 3$ and $\chi N = 160$

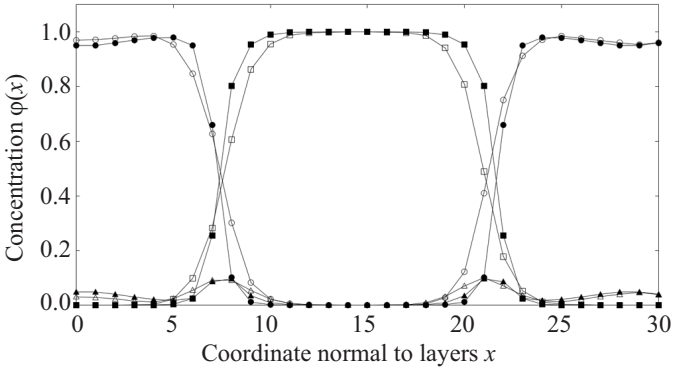

Fig. 4. Density profiles from MC simulations for the 2-32-30 melt: A1 blocks — (Δ), B blocks — (○), A2 blocks — (□) and SCFT calculations: A1 blocks — (▲), B blocks — (●), A2 blocks — (■); T^* = 4 and χN = 120

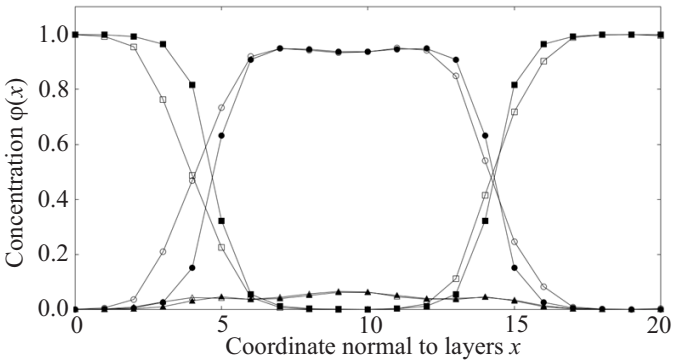

Fig. 7. Density profiles from MC simulations for the 1-16-15 melt: A1 blocks — (Δ), B blocks — (○), A2 blocks — (□) and SCFT calculations: A1 blocks — (▲), B blocks — (●), A2 blocks — (■); T^* = 4.8 and χN = 50

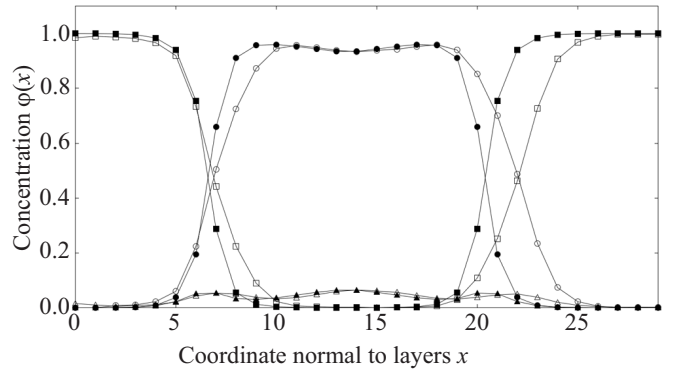

Fig. 5. Density profiles from MC simulations for the 2-32-30 melt: A1 blocks — (Δ), B blocks — (○), A2 blocks — (□) and SCFT calculations: A1 blocks — (▲), B blocks — (●), A2 blocks — (■); T^* = 7 and χN = 69

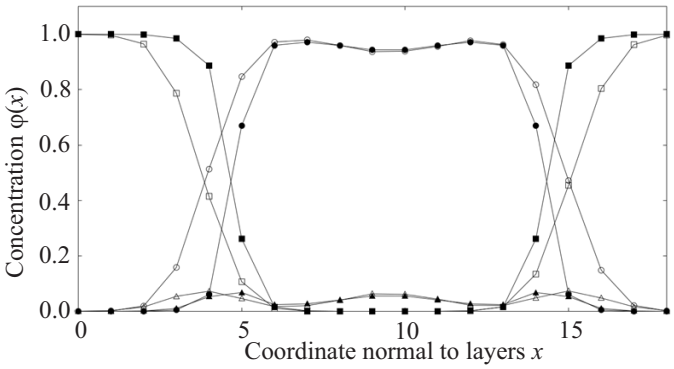

Fig. 8. Density profiles from MC simulations for the 1-16-15 melt: A1 blocks — (Δ), B blocks — (○), A2 blocks — (□) and SCFT calculations: A1 blocks — (▲), B blocks — (●), A2 blocks — (■); T^* = 2.5 and χN = 96

profiles, shown in Figs 3, 4, and 5, from two different methods (MC and SCFT) agree surprisingly well with the single $\chi = 7.5/T^*$ mapping.

This conclusion is also supported by the MC simulations for shorter chains (1-16-15), as indicated in Figs 6, 7, and 8, which present lamellar density profiles for three T^*'s (which are different from those used for the 2-32-30 chains), and the corresponding SCFT data which are expressed in terms of χN.

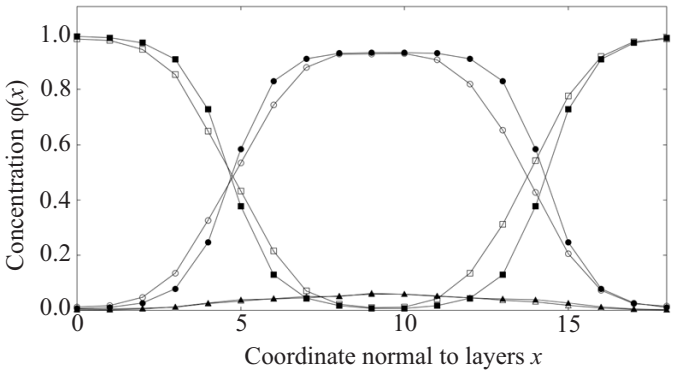

Fig. 6. Density profiles from MC simulations for the 1-16-15 melt: A1 blocks — (Δ), B blocks — (○), A2 blocks — (□) and SCFT calculations: A1 blocks — (▲), B blocks — (●), A2 blocks — (■); T^* = 8.2 and χN = 29

CONCLUSION

Using self-consistent field theory and Monte Carlo simulations we investigated the distribution of A1, B, and A2 segments in the lamellar nanostructure of A1BA2 triblock copolymer melts. We confronted the results obtained from two methods and concluded that as we increased χN, more A1 segments were localized at the interface, and less in the B domain, as expected from previous studies. We also found that the density profiles from two different methods (MC and SCFT) agreed surprisingly well with the single $\chi = 7.5/T^*$ mapping.

ACKNOWLEDGMENTS

Grant DEC-2012/07/B/ST5/00647 of the Polish NCN is gratefully acknowledged. A significant part of the simulations was performed at the Poznan Computer and Networking Center (PCSS).

REFERENCES

[1] Bates F.S., Fredrickson G.H.: *Phys. Today* **1999**, *52*, 32, http://dx.doi.org/10.1063/1.882522

[2] Bailey T.S., Hardy C.M., Epps T.H., Bates F.S.: *Macromolecules* **2002**, *35*, 7007, http://dx.doi.org/10.1021/ma048762s

[3] Takenaka M., Wakada T., Akasaka S., Nishisuji S., Saijo K., Shimizu H., Kim M.I., Hasegawa H.: *Macromolecules* **2007**, *40*, 4399, http://dx.doi.org/10.1021/ma070739u

[4] Hamley I.W.: "Developments in Block Copolymer Science and Technology", John Wiley & Sons, Berlin 2004.

[5] Fredrickson G.H.: "The Equlibrium Theory of Inhomogeneous Polymers", Clarendon Press, Oxford 2006.

[6] Khandpur A.K., Forster S., Bates F.S., Hamley I.W., Ryan A.J., Bras W., Almdal K., Mortensen K.: *Macromolecules* **1995**, *28*, 8796, http://dx.doi.org/10.1021/ma00130a012

[7] Leibler L.: *Macromolecules* **1980**, *13*, 1602, http://dx.doi.org/10.1021/ma60078a047

[8] Matsen M.W., Schick M.: *Macromolecules* **1994**, *27*, 187, http://dx.doi.org/10.1021/ma00079a027

[9] Matsen M.W.: *J. Phys.: Condens. Matter* **2002**, *14*, R21, http://dx.doi.org/10.1088/0953-8984/14/2/201

[10] Fredrickson G.H., Helfand E.: *J. Chem. Phys.* **1987**, *87*, 697, http://dx.doi.org/10.1063/1.453566

[11] Lennon E.M., Katsov K., Fredrickson G.H.: *Phys. Rev. Lett*. **2008**, *101*, 138 302, http://dx.doi.org/10.1103/PhysRevLett.101.138302

[12] Wołoszczuk S., Banaszak M.: *Eur. Phys. J. E.* **2010**, *33* (*04*), 343, http://dx.doi.org/10.1140/epje/i2010-10680-5

[13] Wołoszczuk S., Banaszak M., Spontak R.: *J. Polym. Sci. B: Polym. Phys*. **2013**, *51*, 343, http://dx.doi.org/10.1002/polb.23215

[14] Banaszak M., Koper A., Knychała P., Lewandowski K.: *Acta Physica Polonica A* **2012**, *121* (3).

[15] Dzięcielski M., Lewandowski K., Banaszak M.: *Comput. Methods Sci. Technol*. **2011**, *17* (*1—2*), 17.

[16] Banaszak M., Whitmore M.D.: *Macromolecules* **1992**, *25* (*13*), 3406, http://dx.doi.org/10.1021/ma00039a015

[17] Matsen M.W., Schick M.: *Phys. Rev. Lett.* **1994**, *72*, 2660, http://dx.doi.org/10.1103/PhysRevLett.72.2660

[18] Matsen M.W., Whitmore M.D.: *J. Chem. Phys.* **1996**, *105*, 9698, http://dx.doi.org/10.1063/1.472799

[19] Pakula T. in: "Simulation Methods for Polymers", (Ed. Kotelyanskii M.J., Thedorou D.N.), Marcel-Dekker 2004, Chap. 5.

[20] Knychała P., Dzięcielski M., Banaszak M., Balsara N.: *Macromolecules* **2013**, *46* (*14*), 5724, http://dx.doi.org/10.1021/ma400078y

[21] Banaszak M., Woloszczuk S., Jurga S., Pakula T.: *J. Chem. Phys*. **2003**, *119*, 11 451, http://dx.doi.org/10.1103/PhysRevE.66.031804

[22] Beardley T.M., Matsen M.W.: *Eur. Phys. J. E* **2009**, *32*, 255, http://dx.doi.org/10.1140/epje/i2010-10651-x

[23] Lewandowski K., Knychala P., Banaszak M.: *Comput. Methods Sci. Technol*. **2010**, *16*, 29.